THE AMERICAN MINERALOGIST

JOURNAL OF THE MINERALOGICAL SOCIETY OF AMERICA

Vol. 42 MAY-JUNE, 1957 Nos. 5 and 6

SMYTHITE, A NEW IRON SULFIDE, AND ASSOCIATED PYRRHOTITE FROM INDIANA*

RICHARD C. ERD, HOWARD T. EVANS, JR., AND DONALD H. RICHTER,
U. S. Geological Survey, Washington 25, D. C.

ABSTRACT

X-ray investigation of opaque metallic inclusions in calcite crystals from Bloomington, Indiana, shows the presence of a new iron sulfide, with chemical and physical properties somewhat similar to those of pyrrhotite. This mineral is named smythite in honor of Professor C. H. Smyth, Jr. Both smythite and pyrrhotite occur as very thin hexagonal flakes, 0.05 to 2 mm. in diameter, embedded near the surface of calcite crystals found in geodes in the Harrodsburg limestone. Both are strongly ferromagnetic, and are so similar in appearance and properties that they can be distinguished with certainty only by *x*-ray tests.

Smythite is rhombohedral, space group $R\bar{3}m$ (D_{3d}^5); $a=3.47$ Å; $c=34.5$ Å; $c/a=9.94$; G=4.06 (obs.), 4.09 (calc.). The ideal formula, Fe_3S_4, is derived from study of the structure by *x*-ray techniques. Many other possible structures of similar type were tested and conclusively eliminated on the basis of the Patterson function. Final hexagonal parameters are: $3Fe_1$ in (*b*); $6Fe_2$ in (*c*), $z=0.417$; $6S_1$ in (*c*), $z=0.289$; $6S_2$ in (*c*), $z=0.127$. The structure can be described as consisting of slabs of the pyrrhotite structure stacked loosely on each other in a sheet structure.

Associated pyrrhotite is the strongly ferromagnetic monoclinic phase. Study of the enclosing calcite by the visual method of inclusion thermometry indicates that pyrrhotite and smythite formed at temperatures between 25° and 40° C. and at low pressures. Synthesis of smythite by fusion or from solutions was not successful. Its origin and relationships are discussed.

INTRODUCTION

In June 1950, while making a study of the minerals of Indiana for the Indiana Geological Survey, Erd (1954) discovered what at first seemed to be minute flakes of biotite enclosed by calcite in quartz geodes of the lower Harrodsburg limestone. Study showed the flakes to have the physical properties and *x*-ray power pattern of ferromagnetic monoclinic pyrrhotite. Later, at the U. S. Geological Survey, a second *x*-ray pattern made of similar ferromagnetic material give a unique pattern which was wholly different from that of pyrrhotite. However, even if the then unknown mineral could have been completely separated from the pyrrho-

* Publication authorized by the Director, U. S. Geological Survey.

tite, there still would not have been sufficient material for a chemical or even quantitative spectrographic analysis. Therefore, the crystals were subjected to a crystal structure study which established the ideal composition as Fe_3S_4, and elucidated its crystal chemical relationship to pyrrhotite (Erd and Evans, 1956). To know something of the conditions under which Fe_3S_4 and pyrrhotite originated, fluid inclusions in the enclosing calcite were studied by Richter, using the visual method of inclusion thermometry.

This mineral, Fe_3S_4, is named smythite (smīth′ īt) in honor of Professor Charles Henry Smyth, Jr., economic geologist, petrologist, and for many years lecturer in chemical geology—one of the converging branches of geochemistry (Buddington, 1938). Professor Smyth (1911) was one of the earliest to recognize the occurrence of pyrrhotite in sedimentary rocks.

Occurrence

Smythite and pyrrhotite occur chiefly as inclusions in calcite crystals in quartz geodes found near the base of the lower member of the Harrodsburg limestone, and rarely in geodes at the top of the underlying Edwardsville formation. The lower Harrodsburg limestone is a gray-green, coarsely crystalline, crinoidal limestone with thin beds of shale and siltstone. Geodes in this formation range commonly from 1 to 6 inches but may be more than 2 feet in diameter. The Edwardsville formation consists of interbedded greenish-gray siltstones and shales with geodes that are much smaller and less mineralized than those of the Harrodsburg. These formations mark the top of the Osage series of Mississippian age. The outcrop area, in southwestern Indiana, is far from any igneous rocks and there seems to be little evidence of any hydrothermal activity.

Symthite and pyrrhotite have been found at several localities in Monroe County and as far as 30 miles away near Medora in Jackson County. Pyrrhotite has so far been positively identified at two localities; smythite has been found at four; and either or both (as yet undetermined) are present at five other localities. The greatest abundance of both minerals occurring together was found in a road cut on the east side of State Route 37, two miles north of Bloomington, in the $NW\frac{1}{4}$ $SW\frac{1}{4}$ and $SW\frac{1}{4}$ $NW\frac{1}{4}$ sec. 21, T. 9 N., R. 1 W., Monroe County, and material from this locality was selected as the chief basis for this study. Smythite and pyrrhotite are also found in the abandoned Bloomington Crushed Stone Company quarry, less than a mile south of the first locality. The mineralization of the Harrodsburg in this quarry has been described by Fix (1939).

At the road cut both of the minerals occur as inclusions in calcite, although at other localities smythite or pyrrhotite or both have also been found imbedded in dolomite, barite, or rarely in quartz. Both smythite and pyrrhotite may be found within a single geode but there is a tendency for one or the other to be greatly predominant.

Much has been written concerning the origin of the quartz geodes (Fix, 1939) and the subject cannot be considered here. There is a great variety in the minerals present in the geodes, but a generalized paragenetic sequence can be given for those containing smythite and pyrrhotite. From the rim toward the center, the geodes are composed of cryptocrystalline quartz, often with pyrite or sphalerite on the outer surface; massive, dense, white quartz with black sphalerite; and euhedral doubly terminated quartz crystals. The massive and euhedral quartz, from widely separated localities, contains inclusions of anhydrite. The quartz shell of the geodes is frequently found to be fractured at its base and slightly flattened parallel to the bedding planes of the limestone. This is probably a result of the compressive force developed during intrastratal solution of the enclosing limestone. The fractures have been recemented by additional deposition of silica. Mineralization of the geodes was apparently subsequent to fracturing, for there is no evidence of shattering or distortion in crystals of the later minerals. The sequence of later deposition in the fractured quartz shell is: siderite, dolomite, and calcite of two generations (designated here as I and II) enclosing millerite, barite, smythite, pyrrhotite, and later marcasite and pyrite.

Calcite (I) is cloudy and acute scalenohedral in habit, whereas the crystals of calcite (II) are also scalenohedral, but less acute, and terminate in rhombohedral faces. Calcite (II) is generally 2 to 4 mm. thick. Traces of Mg, Fe, Mn, and Zn were detected microchemically in calcite of both generations. Calcite (II) exhibits a weak pink fluorescence and has a moderately strong yellow thermoluminescence which is most intense at about 220° C. and is extinguished just before the calcite begins to decrepitate.

The included sulfides occur in both generations of calcite and project through, or are on, the surface of calcite (II). With the exception of millerite, they frequently outline the surface of the earlier crystal (Fig. 1). The greatest concentration of smythite, however, is just inside the surface of calcite (I) (Fig. 2). There is a tendency for the platy smythite and pyrrhotite crystals to lie with {0001} parallel to the scalenohedral faces, but there is no other apparent relationship to crystallographic directions in the calcite. Disregarding orientation, the occurrence of the inclusions in the two generations of calcite is similar to Merwin's description (1914) of marcasite and pyrite inclusions in calcite in a geode

from Missouri. The close association between pyrrhotite and calcite suggested possible chemical interaction in their coprecipitation to Smyth (1911). No smythite or pyrrhotite was found in the surrounding rock.

FIG. 1. Smythite inclusions in calcite crystal from the Bloomington Crushed Stone quarry. The sharper scalenohedral habit of the earlier calcite (I) can be seen outlined in phantom by the smythite near the top of the crystal.

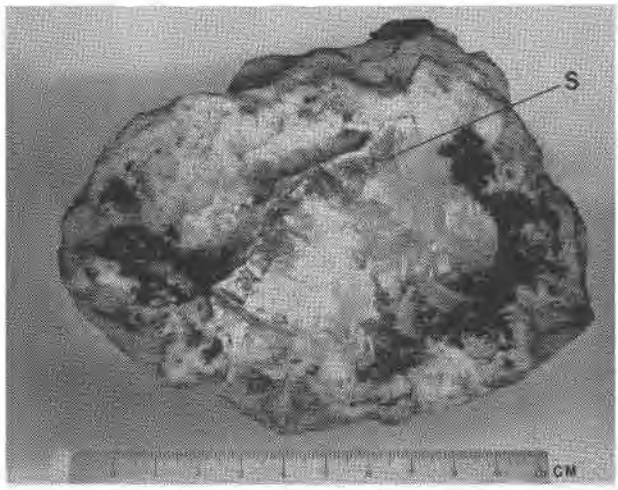

FIG. 2. Calcite in quartz geode containing dark band of smythite inclusions indicated by S. Specimen from road cut on Indiana Highway 37, 2 miles north of Bloomington.

Properties

Physical and optical

The small size of the smythite crystals made measurement of physical properties difficult. Cleavage, which was observed only in the larger flakes, is basal and perfect. The fracture is subconchoidal to smooth. The thin laminae are flexible and elastic. Smythite is soft, being readily scratched with a steel needle. A specific gravity of 4.06 ± 0.03 was obtained by suspension in Clerici solution. Luster on a basal surface is metallic and splendent. Against a white background smythite appears jet black with a tinge of brown; if the basal plane is used as a mirror surface smythite appears light bronze yellow. To obtain the dark-gray streak, several crystals were rubbed across a streak plate with a glass rod. Smythite is strongly ferromagnetic and, since the crystals are attracted edge-on, it is inferred that the direction of easiest magnetization is within the basal plane. The similarity in magnetic properties between smythite and the associated pyrrhotite causes difficulty in obtaining a clean separation.

Optically, smythite is opaque. It seems to be free from inclusions and fresh except for some slight tarnishing and irregular small pitting. In vertically reflected light the color is pinkish cream and not perceptibly different from that of pyrrhotite. Polished prismatic sections are strongly anisotropic, with yellow and blue-gray interference colors, and strongly pleochroic from grayish yellow to reddish brown. Other than the noticeably stronger pleochroism, the optical properties of smythite are similar to those of the associated pyrrhotite.

The cleavage, flexibility, softness, and optical properties of smythite are in accord with the properties characteristic of such other layer-structure minerals as valleriite, sternbergite, covellite, molybdenite, and graphite. Nevertheless, the exceedingly thin flaky habit of the crystals makes it practically impossible to distinguish smythite from the associated pyrrhotite except by an x-ray diffraction test.

Chemical composition and behavior

There was not sufficient material available for quantitative analysis, even by microtechniques, but qualitative microchemical tests showed the major constituents to be iron and sulfur with a minor amount of nickel and traces of copper and zinc. Spindles of smythite and pyrrhotite from Bloomington were examined by means of a curved-crystal x-ray fluorescence spectrometer which showed iron and a small amount of nickel to be present. As the samples were not run against a calibrated standard, the exact atomic ratios are not known with certainty, but smythite seems to contain about half as much nickel as that present in pyr-

rhotite, which is probably less than 1 per cent. Copper and zinc were not detected by this method.

Smythite seems to be more resistant to chemical attack than pyrrhotite. It is slowly soluble in cold dilute hydrochloric or nitric acid and in solutions of potassium hydroxide or silver nitrate. It is very slowly soluble in cold dilute sulfuric acid and is not attacked by carbon disulfide. Smythite left in contact with distilled water was tarnished and pitted after one week, whereas pyrrhotite was attacked to the same extent after three days. Smythite quickly decomposes in a strong (30%) solution of hydrogen peroxide leaving a residue of iron oxide.

When strongly heated, in either a closed or open tube, flakes of smythite warp, curl, and split as they are oxidized to hematite. Smythite remained unchanged when heated in a sealed evacuated tube at 200° C. for one month, but when heated in the enclosing calcite to 400° C. for 18 hours smythite changed completely to pyrrhotite and possibly pyrite although lines of the latter could not be detected in the powder pattern. The pattern was too poor, to determine whether the monoclinic or hexagonal modification of pyrrhotite was formed. The reaction is irreversible. The temperature at which this dissociation begins has not been exactly determined, but a powder pattern of smythite heated in calcite to approximately 290° C. for 18 hours shows diffraction lines of both pyrrhotite and smythite. Some of the smythite crystals, partly exposed by decrepitation of the calcite, oxidized to magnetite, which is evidently the first product of oxidation. In the normal weathering environment smythite alters to goethite. It is only preserved within calcite, dolomite, and none was found in the enclosing rock.

Syntheses and analyses of iron sulfides related to Fe_3S_4

It is of interest that Sidot (1868) claimed to have synthesized ferrosic sulfide (Fe_3S_4) by the reaction of magnetite and hydrogen sulfide at red heat. Attempts made (de Jong and Willems, 1927; Fontana, 1927; Juza, Biltz, and Meisel, 1932; and Michel, 1937) to repeat Sidot's reputed synthesis or otherwise to synthesize Fe_3S_4 with spinel structure, analogous to linnaeite (Co_3S_4), violarite ($FeNi_2S_4$), and polydymite (Ni_3S_4), apparently were unsuccessful, and most of these workers agreed that the existence of ferrosic sulfide with spinel structure is unlikely. Michel (1955, 1956) has recently made a comprehensive study of the reaction between hydrogen sulfide and iron oxides, and reports only FeS as forming in these reactions.

Iron sulfides, or alkali iron sulfides, and their hydrates, with x-ray patterns differing from those of the common iron sulfides, have been prepared from water solutions at ordinary temperatures by Alsen (1923),

Lepp (1954), and Rosenthal (1956), but, so far as we know, none of these compounds gave the powder pattern of smythite. Stevens (1933) prepared similar compounds but gave no *x*-ray data. Lundqvist (1947) synthesized Ni_3S_4 with spinel structure from a water solution, but only repeated and confirmed the work of Allen *et al.* (1912) with the iron sulfides.

Our efforts to synthesize Fe_3S_4, either by fusion or from water solutions, have not been successful; however a systematic program was not attempted. Three different black ferromagnetic compounds, all poorly crystallized as indicated by the diffuse powder diffraction lines, have been obtained from water solutions at room temperature but none shows any relation to smythite. All of these compounds are rapidly attacked by hydrogen peroxide. The common association of pyrrhotite with calcite, in its low-temperature occurrences, suggests the use of calcite to reproduce environmental conditions and also as a surface for nucleation in the synthesis of pyrrhotite or smythite. Weil (1955) emphasized the importance of calcite in his synthetic reproduction of the sulfides found in sediments. Following the directions of Rodgers (1940) for the use of Lemberg's black stain for calcite, but substituting Na_2S for $(NH_4)_2S_x$, we obtained an unidentified product, which also is unrelated to smythite. Powder-diffraction data and details of our experiments are given in the Appendix.

Several analyses reported for pyrrhotite reach, or even exceed, the theoretical 57.14 atomic per cent sulfur in smythite, namely those of Stromeyer (1814) 57.43%, Meunier (1869) 55.79%, and Schulze (reported by Stelzner, 1896) 55.46%. These investigations pre-dated *x*-ray analysis, but the descriptions of the various materials analyzed would indicate that none of the analyses was of smythite. Pyrrhotite from Ertelien, Norway and Petsamo, U.S.S.R., with 56.7 and 55.2 atomic percentages of S, respectively, are regarded by Pehrman (1954) as representing the analysis of material incompletely separated from pyrite or chalcopyrite. He reports three pyrrhotites from Finland as having 54.6, 54.4, and 54.0 atomic per cent S; all exhibited only the monoclinic modification of pyrrhotite in their powder patterns.

Eakle (1922) suggested Fe_3S_4 as the pyrrhotite end member, and Lipin (1946) considered pyrrhotite to be a solid solution of Fe with Fe_2S_3 or Fe_3S_4. However Hägg and Sucksdorff (1933) found the value represented by Fe_4S_5 (55.5 atomic per cent S) as the sulfur-rich composition limit for the pyrrhotite structure. Grønvold and Haraldsen (1952) thought that this value was too high, and that, for temperatures up to 360° C., the limit of the deficiency of iron is close to the composition Fe_7S_8 (53.27 atomic per cent S).

We suggest that smythite represents a stable phase in the Fe-S system, which forms at low temperature and pressure, and which dissociates into pyrrhotite and pyrite or sulfur at a temperature between 200° and 290° C. It is likely that it would occur only in sedimentary rocks or in epithermal deposits.

Crystallography

Morphology

Crystals of smythite range from 0.05 to 1.25 mm. in diameter (most are 0.10 to 0.25 mm. in diameter) and are 1 to 3 microns in thickness. Subhedral irregularly formed crystals are uncommon; most are euhedral platy hexagonal crystals which appear to be a combination of a well-developed base {0001} and a rhombohedron. The prism face was not observed. Even some of these apparently simple crystals, however, were found by *x*-ray study to be twinned on (0001). About half of the crystals are aggregates of intersecting plates. In some, repeated twinning has produced hexagonal plates which have the appearance of being warped.

X-ray powder data

X-ray powder data for smythite and pyrrhotite from Bloomington, Indiana, are given in Table 1. The data for the latter is identical to a pattern of pyrrhotite from Lairdsville, New York, collected by Professor Smyth (Princeton Collections no. 16/74). The smythite pattern was indexed on the values for c and a obtained from the single-crystal study.

Crystal structure and crystal chemistry

A crystal-structure study was made to ascertain the chemical constitution of smythite because of the impractibility of obtaining sufficient material for a chemical analysis. By this means it was possible to establish the chemical formula conclusively as Fe_3S_4, and to elucidate its structural relationship to pyrrhotite.

Buerger precession photographs of the (*hk*.0), (*h*0.*l*), and (*hh.l*) net planes established the lattice as rhombohedral, with the following cell constants:

Space group: $R\bar{3}m(D_{3d}^5)$, $R3m(C_{3v}^5)$, or $R32(D_3^7)$.
Cell dimensions:
rhombodedral: $a=11.66\pm0.03$ Å, $\alpha=17°7'\pm30'$
hexagonal: $a=3.47\pm0.02$ Å, $c=34.5\pm0.2$ Å
Cell volume (hex.): 360 ± 3Å^3
Cell contents (hex.): $3[Fe_3S_4]$
Specific gravity: 4.09 ± 0.04 (calc.); $4.06\pm.03$ (meas.).

A close relationship to pyrrhotite is apparent when the cell constants are compared: β-pyrrhotite (ignoring superstructures) has the (pseudo)

space group $C6_3/mmc$, with $a=3.44$ Å and $c=5.70$ Å ($6c=34.2$ Å). The specific gravity of pyrrhotite (Fe_7S_8) is 4.62. The symmetry and dimensions of smythite place close restrictions on the arrangement of Fe and S atoms in the unit cell. The atoms must all lie on the three 3-fold axes in the cell, but in an identical manner on all three, instead of all Fe on one and all S on the other two as in pyrrhotite. On the basis of these facts, a tentative structure was worked out, keeping in mind the close similarity of smythite and pyrrhotite in nearly all physical and chemical properties.

In Fig. 3, projections are shown of the simple structure of pyrrhotite

TABLE 1. *X*-RAY POWDER DATA FOR SMYTHITE AND PYRRHOTITE FROM BLOOMINGTON, INDIANA

FeKα radiation; 114.6 mm. dia. camera; *d*(obs.) cut-off at 16.0 Å

A. SMYTHITE

hk.l	*d*(calc.)	*d*(obs.)	*I*	*hk.l*	*d*(calc.)	*d*(obs.)	*I*
00.3	11.50	11.5	6	11.12	1.486		
00.6	5.75	5.75	0.5	02.4	1.481		
00.9	3.83	3.82	2	20.5	1.468	1.465	0.5
10.1	2.99	3.00	6	00.24	1.437	1.435	2
01.2	2.96	2.96	0.5	02.7	1.437		
00.12	2.87	2.86	0.5	20.8	1.418	1.427	6
10.4	2.84	2.83	2	02.10	1.377	1.375	0.5
01.5	2.75	2.75	4	20.11	1.354	1.351	0.5
10.7	2.56	2.56	6	01.23	1.342	1.332	0.5
01.8	2.46	2.45	2	02.13	1.308	1.305	2
00.15	2.30	2.29	0.5	11.18	1.286		
10.10	2.26	2.26	6	20.14	1.283	1.280	2
01.11	2.17	2.16	4	00.27	1.279		
10.13	1.988	1.979	7	10.25	1.254	1.254	0.5
00.18	1.917			20.17	1.207	1.204	2
01.14	1.903	1.897	8	02.19	1.158	1.154	0.5
10.16	1.751			00.30	1.150		
11.0	1.736	1.732	10	11.24	1.107		
11.3	1.715	1.715	0.5	01.29	1.105	1.102	4
01.17	1.681	1.687	0.5	02.22	1.084	1.078	0.5
11.6	1.662	1.672	4	20.23	1.061	1.065	0.5
00.21	1.642			00.33	1.045		
11.9	1.581	1.577	0.5	10.31	1.043	1.037	2
10.19	1.554	1.546	0.5	11.27	1.029	1.029	0.5
02.1	1.500			30.0	1.001	1.001	2
20.2	1.497	1.496	0.5	30.3	0.997	0.998	2
01.20	1.496			20.26	0.995		
				30.6	0.987	0.988	0.5

(*Continued on next page*)

B. Pyrrhotite

Note: Calculated lines correspond to hexagonal pseudo-cell; other lines correspond to monoclinic superlattice of β-pyrrhotite.

hk.l	*d*(calc.)	*d*(obs.)	*I*	*hk.l*	*d*(calc.)	*d*(obs.)	*I*
		5.75	4	20.0	1.49	1.488	0.5
		5.29	2	11.2	1.47		
		4.72	2	20.1	1.44	1.439	2
10.0	2.97	2.97	8	00.4	1.42	1.424	6
00.2	2.84	2.84	4	20.2	1.32	1.320	4
		2.70	0.5	10.4	1.28	1.286	0.5
10.1	2.64	2.64	9			1.230	0.5
		2.27	4	20.3	1.17	1.174	0.5
		2.21	2			1.138	0.5
		2.16	2			1.105	0.5
10.2	2.06	2.06	10	11.4	1.095	1.100	4
		2.01	0.5			1.065	0.5
		1.946	0.5	21.2	1.045	1.049	2
		1.914	0.5			1.043	4
11.0	1.72	1.717	8	30.0	.991	0.992	6
		1.632	0.5				
10.3	1.60	1.606	2				

along the *c* and *a* axes. Also shown is the smythite structure as it was finally deduced, projected along the *a* axis. With reference to this figure, the following description of the solution of the structure may be more clearly understood.

Starting at the origin (symmetry center) of the rhombohedrally centered hexagonal cell, a model structure was developed by building a pyrrhotite structure upward until symmetry restrictions interfered. Thus, the smythite cell was found able to accommodate a pyrrhotite structure four sulfur and three iron layers deep, but beyond this point, a shift in the structure is required because of the rhombohedral lattice node at $\frac{2}{3}\frac{1}{3}\frac{1}{3}$. Starting anew at this point, a second slab of pyrrhotite structure was erected until the point $\frac{1}{3}\frac{2}{3}\frac{2}{3}$ was reached, where another shift is required. In this way, the pyrrhotite structure was found to fit the smythite unit cell, but with shifts in the structure after each fourth layer of sulfur atoms along the *c* direction. The best way to account for these shifts seemed to be to assume that the iron atoms that would be coordinated between the shifted sulfur layers are actually omitted, thus giving rise to a layer structure consisting of pyrrhotite slabs loosely stacked on each other in a rhombohedral mode. This hypothesis led directly to the formula Fe_3S_4, which was subsequently confirmed by density measurement. The symmetry of the proposed structure was then

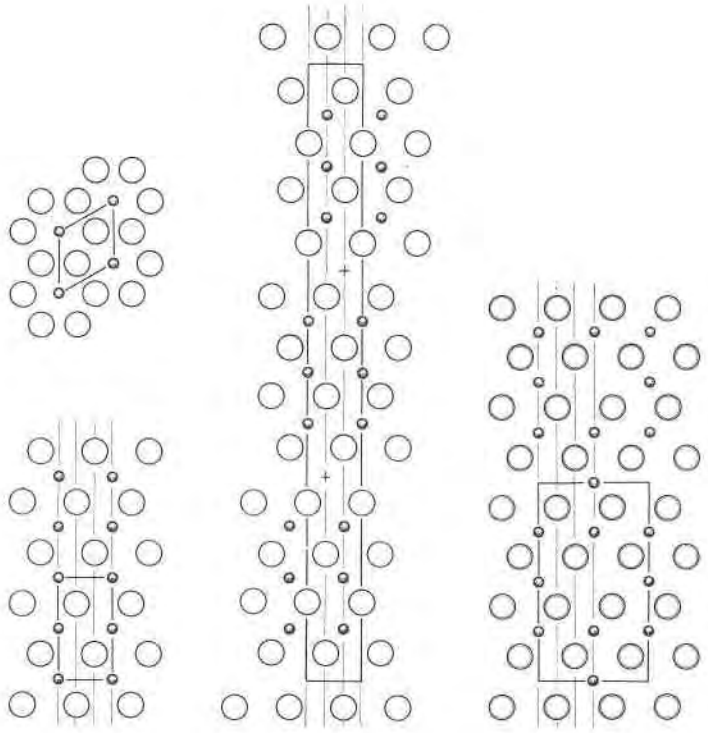

(*a*) (*b*) (*c*)

FIG. 3. Crystal structures of smythite and related structures. (*a*) Pyrrhotite structure projected along hexagonal *c* axis (top) and *a* axis (bottom). (*b*) Smythite structure projected along hexagonal *a* axis. (*c*) Fe_3Se_4 structure projected along pseudohexagonal *a* axis. Fe atoms represented by small shaded circles, S atoms by large single circles, Se atoms by large double circles. Three-fold axes represented by vertical lines.

assumed to be $R\bar{3}m$, and coordinates assigned to the atoms as follows: $3Fe_1$ in (*b*) with $z=\frac{1}{2}$; $6Fe_2$ in (*c*) with $z=5/12$; $6S_1$ in (*c*) with $z=7/24$; $6S_2$ in (*c*) with $z=3/24$.

To test this structure, intensities were measured for 35 ($h0.l$) reflections, using the Buerger precession photograph shown in Fig. 4. It is apparent from this pattern that the intensities could not be measured to the usual standards of accuracy, since the photograph shown is the best that could be obtained from the available crystals. Intensities were estimated by comparison with a calibrated series of spots made from another crystal. The intensities were multiplied by a correction factor of the form $(w+r\tau)/w$ in an attempt to counteract the smearing effect on the spots resulting from the angular distortion of the crystal which is

apparent from the photograph. In this expression, w represents the normal spot diameter, r the distance of the spot from the center of the pattern, and τ the angle of distortion in radians. The Lorentz-polarization correction was estimated by means of a Waser chart (Waser, 1951). No correction was made for absorption. The crystal was approximately 0.2 mm. across and 5 microns thick, and required 72 hours exposure, using unfiltered MoK radiation at 50 kv and 20 ma to give the pattern shown.

The first trial of the hypothetical structure gave a reliability factor of

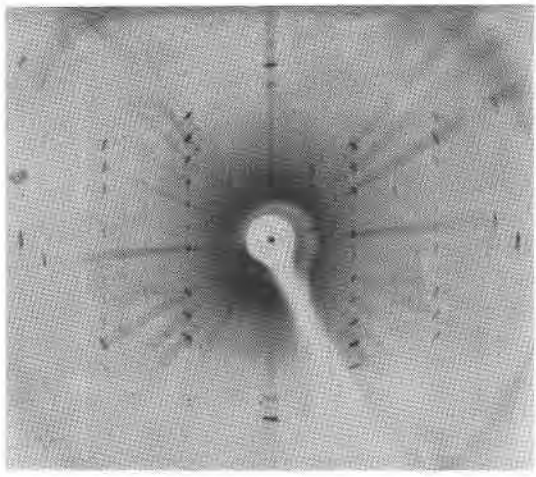

FIG. 4. Buerger precession photograph of ($h0.l$) net plane of smythite. MoK radiation, unfiltered.

20.5%, which was taken as strong evidence of the correctness of the structure. Nevertheless, it was recognized that many other structures could be postulated which satisfy the structural restrictions referred to earlier, plus other requirements that can be defined. Allowing both octahedral and prismatic coordination for iron (the latter being exemplified by molybdenum in MoS_2), it was found that 25 different model layer structures could be built which would fit the unit cell with space group $R\bar{3}m$ or $R3m$. The Patterson function $P(0,z)$ was evolved for each of these and compared with the Patterson function calculated from the observed intensities. A good match was found for only one of the 25 structures, the one corresponding to that already described. Reliability factors calculated for some of these structures ranged from 30 to 45%. It seems unnecessary to consider any structures further, aside from the one described.

The postulated structure was refined by least squares analysis (using

unweighted values of ΔF), giving final parameters listed below:

Space group: $R\bar{3}m(D_{3d}^5)$
Parameters:
$3Fe_1$ in (b), ($z=\frac{1}{2}$)
$6Fe_2$ in (c), $z=0.4171\pm0.0006$
$6S_1$ in (c), $z=0.2888\pm0.0010$
$6S_2$ in (c), $z=0.1270\pm0.0010$

This structure, with a temperature factor e^{-Bs^2} applied to the calculated

TABLE 2. COMPARISON OF OBSERVED AND CALCULATED STRUCTURE FACTORS OF SMYTHITE

h0.l	*F*(calc.)	*F*(obs.)	*h0.l*	*F*(calc.)	*F*(obs.)	*h0.l*	*F*(calc.)	*F*(obs.)
00.30	−48	A	10.28	−3	A	20.17	83	97
00.27	−51	51	10.25	−58	41	20.14	108	120
00.24	197	201	10.22	43	58	20.11	−108	74
00.21	−28	51	10.19	−48	62	20.8	26	53
00.18	−31	32	10.16	17	44	20.5	−45	48
00.15	−43	44	10.13	−167	152	20.2	38	34
00.12	42	46	10.10	145	120	20.$\bar{1}$	−86	81
00.9	−59	53	10.7	143	118	20.$\bar{4}$	−19	34
00.6	−76	N	10.4	−28	32	20.$\bar{7}$	103	92
00.3	−78	N	10.1	−126	118	20.$\bar{10}$	104	79
00.0	426	—	10.$\bar{2}$	57	55	20.$\bar{13}$	−122	109
			10.$\bar{5}$	−64	84	20.$\bar{16}$	13	A
			10.$\bar{8}$	35	77			
			10.$\bar{11}$	−151	120			
N=not measured			10.$\bar{14}$	145	159			
A=absent			10.$\bar{17}$	105	106			
			10.$\bar{20}$	−40	A			
$R=0.186$			10.$\bar{23}$	−91	55			
$B=0.90\pm0.3$ Å^2			10.$\bar{26}$	28	A			
			10.$\bar{29}$	−33	44			

structure amplitudes in which $s=(\sin\theta)/\lambda$ and $B=0.90$ Å^3, gives a reliability factor of 18.5%. No significance can be attached to the value of B, since it depends in large measure on the choice of w and τ used in the expression applied to correct intensities for pattern distortion as described above. Final calculated and observed structure factors are listed in Table 2.

A Fourier synthesis of the electron density in smythite along one three-fold axis was carried out by means of the function

$$= \frac{1}{A} \Sigma F(h0.l) \cos 2\pi lz$$

and the result is shown on a relative scale in Fig. 5. A synthesis is also shown in which the values of F in the series are replaced by ΔF. The peaks correspond well with the postulated atomic positions, and there are no features that justify special interpretation.

The structure is entirely consistent with the normal pyrrhotite structure, except for the layer feature. This consistency is demonstrated by

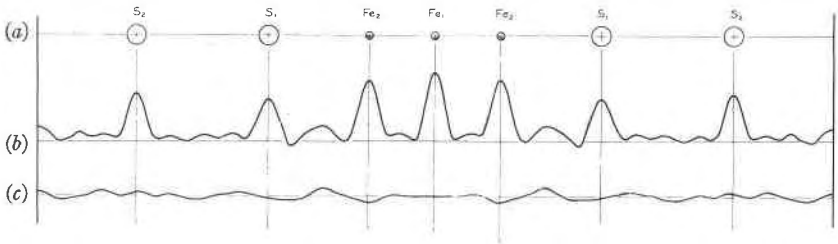

FIG. 5. Fourier synthesis of electron density in smythite. (*a*) Position of atoms on one three-fold axis. (*b*) Electron density on arbitrary scale along the three-fold axis. (*c*) Electron density residual along the three-fold axis on same scale as (*b*).

the interatomic distances given in Table 3 and Fig. 6. Standard deviations shown in the table were computed from the standard deviation of the structure amplitudes. Evidently, the structure itself calls for no special comment.

Two further observations on the crystallography of smythite may be noted. First, there is evidence on the photograph of Fig. 4 of twinning on (00.1). Such twinning is to be expected from an uncertainty in the direction of rhombohedral stacking resulting from the very slight energy difference that must obtain between rhombohedral and hexagonal stacking of the layers. Second, there is evidence on the photograph of a superlattice based on the rhombohedral lattice described, which is also probably rhombohedral but with the a axis and possibly the c axis doubled. There is no way in which variations in the stacking sequence of the layers could double the a axis; therefore, there is a strong possibility that the superstructure results from the ordering of vacancies resulting from a small deficiency of iron, as in the case of β-pyrrhotite.

It is of interest to compare the structure found for Fe_3S_4 with that recently proposed for a new synthetic compound, Fe_3Se_4, described by Okazaki and Hirakawa (1955). According to these authors, Fe_3Se_4 is monoclinic with space group $P2/m(C_{2h}^1)$, $a=6.16_7$ Å, $b=3.51_7$, $c=11._7$ and $\beta=92.0°$. The structure is described as being directly derived from a distorted pyrrhotite structure with one out of every four Fe atoms absent. The atoms are arranged in the unit cell described with 1 Fe in (*e*)

at $\frac{1}{2}\frac{1}{2}0$; 1 Fe in (*c*) at $00\frac{1}{2}$; 2 Fe in (*l*) at $\frac{1}{2}\frac{1}{4}\frac{1}{2}$, $\frac{1}{2}\frac{3}{4}\frac{1}{2}$; 2 Fe in (*i*) at $0\frac{1}{4}0$, $0\frac{3}{4}0$; and vacancies at the sites (*a*) at 000, and (*h*) at $\frac{1}{2}\frac{1}{2}\frac{1}{2}$. As shown in Fig. 3*c*, this arrangement leads to rows of three Fe atoms along the *c* axis, but they are staggered with respect to each other in the hexagonal close-packed sulfur framework, and consequently a layer structure does not result as in smythite.

TABLE 3. INTERATOMIC DISTANCES IN SMYTHITE

(See Fig. 6)

Vector	Atoms	Smythite	Other structures
A	Fe_1 to Fe_2	2.86±0.02 Å	2.84 Å (pyrrhotite)
B	Fe_1 to S_2	2.42±0.04	2.44 (pyrrhotite)
C	Fe_2 to S_2	2.50±0.04	
D	Fe_2 to S_1	2.42±0.04	
E	S_2 to S_2	3.39±0.05	3.46 (pyrrhotite)
F	S_1 to S_2	3.48±0.05	
G	S_1 to S_1	3.67±0.05	3.67 (molybdenite)
H	Fe_2 to S_2	4.43±0.07	
J	S-S (*a* axis)	3.47±0.01	3.44 (pyrrhotite)

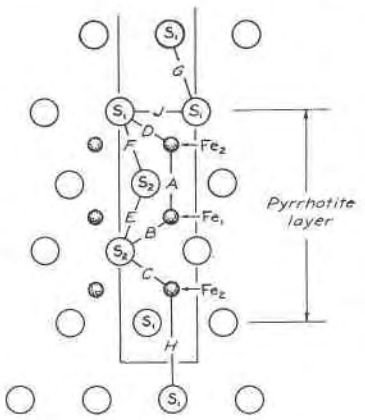

FIG. 6. Atom types and interatomic vectors in smythite.

CONDITIONS OF FORMATION AS INDICATED BY FLUID INCLUSIONS

It is clear that smythite and pyrrhotite were formed at the same time and under the same pressure and temperature conditions as the enclosing calcite. Fluid inclusions in coarsely crystalline transparent calcite, containing smythite, from two widely separated localities were investigated by the visual (Sorby) method of inclusion thermometry. More than 200

fluid inclusions were studied in six polished thick sections and numerous thin cleavage plates.

Two distinct types of fluid inclusions, based on physical appearance and orientation, were observed in the calcite. Inclusions of type 1 are flat, usually with an irregular outline and probably occur on the $\{10\bar{1}1\}$ planes. Some are in the form of complex or multiple parallelepipeds with the acute plane angles approximately those of the cleavage rhombohedron of calcite, viz. 75°. The inclusions range in size from less than 0.02 mm. to 0.10 mm., the smaller being more abundant. Type 2 are very small ($<$0.002 mm.) tubular and ovoid-shaped inclusions occurring in short gently curving and intersecting planes; hundreds are present in one minute plane.

The inclusions, whether of type 1 or 2, are all one-phase at room temperature. When heated to temperatures above 225° C., and then cooled, a large amount of vapor phase is formed due to leakage of liquid along fractures or parted cleavage plates. With a linear heating rate of approximately 20° C./minute the calcite decrepitates at 265° C. Furthermore, when cooled with liquid nitrogen the calcite also fractures, due in this case to the expansion and relative incompressibility of the solid phase formed. The inclusion fluid, therefore, is undoubtedly liquid. Attempts to separate a vapor phase in the inclusions by cooling to 1° C., in a microscope-mounted ice bath, were unsuccessful in all but four of the larger type-1 inclusions. Assuming that pressure-temperature conditions in the inclusion were the same as those in the growth solution, and the interfacial tension was negligible, a vapor phase should form on cooling prior to the temperature of maximum density, unless, of course, the calcite formed at that temperature (4° C.). However, inasmuch as the volume change is only -0.60% when cooled from 35° C. to 4°C. (the temperature of maximum density of pure water), it is very possible that the interfacial tension between inclusion fluid and calcite is strong enough to prevent contraction of the liquid and the formation of a vapor phase. This is further substantiated by the fact that only the larger inclusions, which have a relatively small surface area per unit volume, become two-phase on cooling below room temperature.

After removal from the cooling chamber, the four larger inclusions, in which a vapor phase was formed, completely filled with liquid at temperatures of 27, 31, 35, and 38° C. The three higher filling temperatures were determined in a microscope-mounted heating chamber. It is probably safe to assume, therefore, that all the inclusions, especially those of type 1, would have filling temperatures somewhere within this range if the liquid on cooling had formed a vapor phase.

The determination of formation temperatures of minerals from fluid

inclusion studies are based on a number of important assumptions. Although these assumptions, which were made in part by Sorby (1858) in his classical work, have been considered in detail in recent years by many workers (Ingerson, 1947; Bailey and Cameron, 1951; Cameron, Rowe, and Weis, 1953; and Smith, 1953), it is necessary in each individual investigation to review the assumptions, in order to evaluate fully all experimental and other data. Although all assumptions, which are discussed below, cannot be rigorously proved to be correct, they do allow very probable geothermometric conclusions.

(1) The inclusions were completely filled with liquid at the time of formation and have not lost or gained liquid since that time.

The solutions responsible for the deposition of calcite and associated minerals in the geodes were without much doubt aqueous, and, as evidenced by the degree of filling of the inclusions, probably completely filled the inclusions at the time of entrapment. Skinner (1953) after an investigation of fluid inclusions in quartz, concluded that high-pressure differentials between inclusion fluids and host-crystal media can force liquid into, or out of, fluid inclusions, probably along lineage boundaries. In their reply to Skinner's paper, Richter and Ingerson (1954) showed that liquid could not be forced out of primary fluid inclusions (other than leakage along fractures) in quartz and calcite under the conditions cited by Skinner. They contended, therefore, that the single crystal of quartz studied by Skinner is exceptional in some of its properties and further work is necessary before this basic assumption is invalidated. There is no evidence to suggest that liquids have migrated from the inclusions, and furthermore, consideration of concordant geological evidence of a low temperature-pressure environment, makes it seem doubtful if pressure differentials ever existed that could force liquid into the inclusions.

(2) The inclusions contain an aqueous solution with negligible amounts of CO_2 or other gases.

The inclusion liquid, in the inclusions where a vapor phase was observed, has a low viscosity and exhibits Brownian movement. The single vapor phase when cooled to 1° C. does not separate any additional phases, nor on heating above 31 ° C. is there a marked increase in the size of the vapor bubble, as would be expected if significant amounts of CO_2 were present. Unfortunately attempts to determine the freezing point of the liquid were unsuccessful. It is inferred, by analogy with other analyzed inclusion fluids, and admittedly there are only a few, that the liquid is a dilute aqueous solution (5–10%) of K, Na, and Ca salts. Specimens were

crushed and leached with distilled water, but the concentration of Cl^- or SO_4^{-2} ions was too low to be detected by this method.

(3) The volume of the inclusion has remained constant.

The solubility of the calcite in the inclusion fluid at temperatures in the range of 0–35° C. and pressures up to 100 atmospheres is probably negligible. A 0.5 M NaCl solution at 24° C. under a CO_2 pressure of 50 bars dissolves less than 1% of calcite (Miller, 1952). At considerably lower, or zero, CO_2 pressures, which would be comparable to the system under investigation, the solubility would be much less.

At temperatures and pressures in the range given above, the compressibility of water is more than 30 times that of calcite (Birch, 1942), and therefore a change in volume of the inclusion cavity, due to their relative compressibilities, would also be negligible.

(4) The fluid inclusions are primary or can be distinguished from secondary or subsequent inclusions.

Inclusions of type 1 are apparently primary. They probably occur on the $\{10\bar{1}1\}$ planes, and although very irregular in outline, do in some cases tend to have a negative crystal shape. Constancy of the degree of filling of the inclusions (all one-phase at room temperature) also indicates a primary origin. It is conceivable, though, that these inclusions are the result of later solutions, reflecting a lower temperature environment, which under pressure penetrated the calcite along these planes. Inasmuch as liquid cannot be forced out of the inclusions, unless through fractures, it seems improbable that it could be forced into the inclusions, under the very low pressure differentials that might have existed after crystallization. Inclusions of type 2, which occur in gently curving and intersecting planes in random distribution, apparently formed subsequently to the calcite, but under similar pressure-temperature conditions.

(5) The pressure at the time of formation was low or its magnitude can be estimated.

The available data indicate that the overburden at the time of formation was less than 1000 feet, equivalent to a maximum pressure of 85 bars if lithostatic, 30 bars if hydrostatic, or much less if the calcite was only under the vapor pressure of the mineralizing solutions. However, since the calcite formed in hollow geodes (Fig. 2) or in vugs, the crystals were not under lithostatic pressure during, or subsequent to, formation. Whatever the case, the pressure was negligible and no temperature correction is necessary.

Thus the fluid inclusions in calcite from geodes in the Harrodsburg

limestone indicate crystallization at temperatures between 25 and 40° C. Pressures during crystallization were correspondingly low, and definitely not exceeding a maximum of 30 bars.

Some evidence of environmental conditions during formation of the geodes is furnished by the presence of apparently primary inclusions of anhydrite in the massive quartz forming the geode shell and in the later quartz euhedra. According to MacDonald (1953) anhydrite is precipitated from natural sea water above a minimum temperature of about 34° C. If the anhydrite were deposited from a solution containing only $CaSO_4$, this temperature would be 40° C. Pressure, at least up to 100 bars, has little effect on this temperature. Regardless of whether the quartz and anhydrite were precipitated from a sea of Mississippian age or from later ground water solutions (evidence favors the latter), the lower temperature limit for the formation of anhydrite agrees well with the range of temperature of formation of the calcite given above. No upper limit can be established, but unless unusual conditions prevailed, there was probably no significant change in the temperature conditions between the crystallization of the quartz and anhydrite and the subsequently deposited calcite, smythite, and pyrrhotite.

Pyrrhotite

The pyrrhotite associated with smythite is the strongly ferromagnetic, monoclinic modification. The powder pattern of this material, shown in Table 1, agrees very well with that of the synthetic β_3-phase, Fe_7S_8, prepared by Grønvold and Haraldsen (1952). As was previously stated, pyrrhotite from Bloomington was determined to contain nickel by means of x-ray fluorescence analysis. Crystals of pyrrhotite are euhedral hexagonal plates and range in size from a diameter of 0.05 mm. to about 2 mm. or nearly double the size of the largest smythite crystals. It is difficult to distinguish between the associated pyrrhotite and smythite, but pyrrhotite appears to be more bronze and less black against a white background. It is brittle and plates in calcite are bent or broken and not curved as are those of smythite. The color in vertically reflected light is pinkish cream; anisotropism of prismatic sections is strong with yellow and blue-gray interference colors; weakly pleochroic from pale to brownish yellow.

The occurrence of this low-temperature pyrrhotite seems, in most respects, similar to other such reported occurrences of pyrrhotite from sedimentary rocks. Many of these have been summarized by Rosenthal (1956), but several others should be mentioned. Julien (1886) described "amorphous" black iron sulfide from the marshes of New Jersey and elsewhere, and Andrussev (1897) also described globules of ferrous sulfide

from muds of the Black Sea. Blatchley (1903) mentioned black flakes of iron sulfide in some of the strongly sulfurated springs and wells of Indiana. Pyrrhotite was specifically identified by Smyth (1911) as occurring in the upper part of the Clinton formation of Silurian age, near Lairdsville and at Clinton, New York. Here it is associated with calcite and dolomite in quartz-lined cavities in calcareous hematitic sandstone. Dale (1953) has also described this occurrence and has done experimental work on the pyrrhotite. The powder pattern of pyrrhotite from Lairdsville is identical with that of pyrrhotite from Bloomington shown in Table 1. Smythite was not found in a specimen (Princeton Collections no. 16/74) from this locality. Davies (1912) found pyrrhotite as an authigenic mineral in the Arctic Bed, a marsh deposit of late Pleistocene age, in the Lea Valley, Ponder's End, Middlesex, England. Hatch and Rastall (1923) noted pyrrhotite as occurring in shales. Milner (1929) mentioned several reported occurrences of pyrrhotite as an authigenic mineral in sediments and he (1940) identified the mineral in various British soils. Rubey (1930) described pyrrhotite from a pyritic and gypsiferous limestone, the Greenhorn formation of Late Cretaceous age, in the Black Hills region of Wyoming and Montana. Tamayo (1955) described authigenic low-temperature pyrrhotite, intimately associated with pyrite and marcasite, transecting calcareous foraminiferal shells and coarsely crystalline calcite in the lower Tortonien clay of Miocene age from many localities in the "gypsum-sulfur" regions of Sicily. Stanton (1955) reported pyrrhotite and chalcopyrite in tuffaceous carbon-bearing shales, the uppermost members of the Triangle Creek Group which underlie the Rockley Volcanics of Late Ordovician (?) age, in the Rockley district, New South Wales. The pyrrhotite, according to Stanton, resulted from metamorphism of FeS_2 which was originally deposited by bacterial action during sedimentation.

Unfortunately *x*-ray powder data have not been given for these occurrences. It would be interesting to know whether the strongly ferromagnetic monoclinic or the weakly ferromagnetic hexagonal pyrrhotite is the more common in sedimentary rocks. The study of Kiskyras (1950) indicates that the strongly magnetic form predominates in low-temperature material, but since both monoclinic and hexagonal phases can be formed and are stable at room temperature (Allen *et al.*, 1912; Grønvold and Haraldsen, 1952), either might be expected to occur in this environment depending upon the concentration of sulfide ion present. Oftedahl (1955), by optical methods, detected low-temperature pyrrhotite in a black, bituminous, shale of Cambrian age at Oslo, Norway. However, he could not obtain an *x*-ray pattern of either hexagonal or monoclinic pyrrhotite from this material. A magnetic pyrrhotite, reported from

clays of Lower Jurassic age of the German-Holland border region by Hoffman (1948), has a composition close to $Fe_{11}S_{12}$ which suggests that it might be the hexagonal phase, but again, *x*-ray data are not available.

Origin

Some clues as to the origin of smythite and pyrrhotite emerge from the preceding discussions. The sulfides are epigenetic, being deposited in the geodes after they were fractured; they crystallized simultaneously with the enclosing calcite (there is no evidence of replacement) which suggests that the depositing solution was neutral or weakly alkaline; they were formed in a trapped solution supplied with mineralizing ions by percolation and probably slow diffusion through pores and crevices in the surrounding rock and geode shell; the temperature during formation was between 25 and 40 ° C. and the pressure was low.

The source of iron seems most likely to have been FeS_2, disseminated in the lower Harrodsburg limestone and Edwardsville formation, which was oxidized to produce iron sulfate as an end product. The sulfur may also have been supplied by the disseminated FeS_2, for Mapstone (1954) found experimentally that both FeS and H_2S are formed as intermediate products in the weathering of pyrite by oxidation. Another possible source of sulfur is as H_2S transported by ground water and derived from buried organic matter, including petroleum, or from connate waters carrying the gas in solution. Blatchley (1903) mentioned several wells in the area containing dissolved H_2S. The total amount of iron and sulfur available to form smythite and pyrrhotite was small in any event, as they are present only in minute quantities.

Smythite and pyrrhotite seem to have preferentially nucleated directly on the growing calcite rather than to have grown in the solution in the geode and indiscriminately settled on calcite, dolomite, and quartz. Some crystals of both pyrrhotite and smythite can be found on, and in, other minerals, but the preponderance of the sulfides in the calcite and the tendency toward orientation supports this hypothesis.

Acknowledgments

We thank Dr. Brian H. Mason and Dr. Gunnar Kullerud for helpful comments; Dr. Harry H. Hess and Princeton University for their loan of pyrrhotite from New York; Dr. George S. Switzer and the U. S. National Museum for their loan of valleriite from Sweden; and Dr. Fredrik Grønvold for his donation of samples of synthetic and natural pyrrhotites.

We are indebted to our colleagues at the U. S. Geological Survey; to George T. Faust for helpful advice; to Fred A. Hildebrand for compari-

sons of powder patterns of hexagonal and monoclinic phases of pyrrhotite; to Isadore Adler for the analyses by *x*-ray fluorescence spectrometry; and to Charles Milton for an examination of a polished section of smythite.

APPENDIX

Experimental Attempts to Synthesize Smythite

Attempts to synthesize smythite from various systems yielded no products which could be related to smythite, but it was felt that the experiments were of sufficient interest to warrant brief description. *X*-ray powder data for the solid phases obtained are given in Table 4.

Table 4. *X*-Ray Powder Data for Synthetic Products

FeKα radiation; 114.6 mm. dia. camera

Expt. 1		Expt. 2		Expt. 3	
d(obs.)	*I*	*d*(obs.)	*I*	*d*(obs.)	*I*
6.3	2	8.1	10	7.0	7
3.49	6	6.1	4	5.34	6
2.98	6	5.37	9	4.57	4
2.32	4	4.02	4	2.89	6
1.84	7	2.94	4	2.31	2
		2.76	6		

Note: all lines are broad.

Experiment 1. A black magnetic opaque material and pyrite were formed from a dilute solution of $FeSO_4$ saturated with H_2S and brought to a pH of 8.5 with NH_4OH. The precipitate was leached with water, dried, and allowed to stand 45 days. No change was observed in the powder pattern after this time, but when heated to 170° C. the material gave a pattern of hematite, marcasite, and pyrite. The original product was also prepared in a variety of ways such as treatment of siderite with Na_2S, H_2S, and dilute H_2SO_4.

Experiment 2. A black magnetic opaque precipitate resulting from the reaction of solutions of $FeCl_3$ and Na_2S at a pH of 11. The product was leached with water and was still moist when rolled into a powder spindle. Material allowed to dry in air completely oxidized to goethite in a few days.

Experiment 3. Some of the product of experiment 2 was gently warmed, almost to dryness, and compressed in a steel mortar. This gave a material

which was more strongly ferromagnetic and apparently more stable than that of experiment 2 as it only completely oxidized to goethite after about one month. This material is identical with the black stain formed on calcite by Lemberg's test.

References

Allen, E. T., Crenshaw, J. L., Johnston, John, and Larsen, E. S. (1912), The mineral sulphides of iron, with crystallographic study: *Am. Jour. Sci.*, 4th ser., **33,** 169–236.

Andrussov, N. (1897), La Mer Noire: 7e *Congrès Géol. Internat., Guide des Excursions,* fasc. **29,** 13 p.

Alsen, Nils (1923), Vorlaüfige Mitteilung über eine Untersuchung der Kristallstrukturen von FeS und NiS: *Geol. Fören. Stockholm. Förh.*, **45,** 606–609.

Bailey, S. W. and Cameron, E. N. (1951), Temperatures of mineral formation in bottom-run lead-zinc deposits of the Upper Mississippi Valley, as indicated by liquid inclusions: *Econ. Geol.*, **46,** 626–651.

Birch, Francis (1942), Handbook of physical constants: (Francis Birch, ed.) *Geol. Soc. America Spec. Paper*, **36,** 325 p.

Blatchley, W. S. (1903), The mineral waters of Indiana: *Indiana Dept. Geol. and Nat. Res.*, 26th Ann. Rept., 1901, 18, 88–89.

Buddington, A. F. (1938), Memorial to Charles Henry Smyth, Jr.: *Geol. Soc. America Proc.*, (1937),195–202.

Cameron, E. N., Rowe, R. B., and Weis, P. L. (1953), Fluid inclusions in beryl and quartz from pegmatites of the Middletown District, Connecticut: *Am. Mineral.*, **38,** 218–262.

Dale, N. C. (1953), Geology and mineral resources of Oriskany quadrangle (Rome quadrangle): *New York State Museum Bull.*, **345,** 78–79.

Davies, G. M. (1912), The mineral composition of the Arctic Bed at Ponder's End: *Geol. Soc. London Quart. Jour.*, **68,** 247–248.

De Jong, W. F., and Willems, H. W. V. (1927), Die Verbindungen Fe_3S_4, Co_3S_4, Ni_3S_4, und ihre Struktur: *Zeits. anorg. u. allg. Chemie*, **161,** 311–315.

Eakle, A. S. (1922), Massive troilite from Del Norte County, California: *Am. Mineral.*, **7,** 77–80.

Erd, R. C. (1954), The Mineralogy of Indiana, Master's Thesis Indiana University, 170 p.

——— and Evans, H. T., Jr. (1956), The compound Fe_3S_4 (smythite) found in nature: *Jour. Am. Chem. Soc.*, **78,** 2017.

Fix, G. F. (1939), Mineralization in the Harrodsburg limestone: *Indiana Acad. Sci. Proc.* (1938), **48,** 124–128.

Fontana, C. (1927), Sulla indentità di struttura cristallina dei composti Fe_3S_4 e FeS: *Atti Accad. Lincei*, 6th ser., **5,** 579–581.

Grønvold, Fredrik and Haraldsen, Haakon (1952), On the phase relations of synthetic and natural pyrrhotites ($Fe_{1-x}S$): *Acta Chemica Scandinavica*, **6,** 1452–1469.

Hägg, Gunnar and Sucksdorff, Ingrid (1933), Die Kristallstruktur von Troilit und Magnetkies: *Zeits. physikal. Chemie*, **B22,** 444–452.

Hatch, F. H. and Rastall, R. H. (1923), The petrology of the sedimentary rocks, 2d ed., 201, 217, George Allen and Unwin, Ltd., London.

Hoffman, Karl (1948), Vorkommen von Einfach-Schwefeleisen (Magnetkies) in Sedimentgesteinen: *Erdöl u. Kohle*, **1,** 231–232.

Ingerson, Earl (1947), Liquid inclusions in geologic thermometry: *Am. Mineral.*, **32,** 375–388.

Julien, A. A. (1886), The microscopical structure of the iron pyrites: *New York Microscopical Soc., Jour.*, **2,** 85–96.

JUZA, ROBERT, BILTZ, WILHELM, AND MEISEL, KARL (1932), Das Zustandsdiagram Pyrit, Magnetkies, Troilit and Schwefeldampf, beurteilt nach Schwefeldampfdrucken, Röntgenbildern, Dichten und magnetischen Messungen: *Zeits. anorg. u. allg. Chemie*, **205**, 273–286.

KISKYRAS, D. A. (1950), Untersuchungen der magnetischen Eigenschaften des Magnetkies bei verschiedenen Temperaturen in besondern Hinblick auf seine Enstehung: *Neues Jahrb. Min. Geol., Abh.*, **80**, A, 297–342.

LEPP, HENRY (1954), An experimental study of interconversions among iron carbonates, oxides, and sulfides: thesis at University of Minnesota, 108 p. Abstract in *Dissertation Abstracts*, **14**, 983.

LIPIN, S. V. (1946), On the nature of pyrrhotite and troilite: *Soc. russe mineralogie Mem.*, **75**, 273–284.

LUNDQVIST, DICK (1947), *X*-ray studies on sulphides of nickel and iron obtained by precipitation from water solutions: *Arkiv for Kemi, Mineralogi och Geologi*, **24A**, no. 23, 7 p.

MACDONALD, G. J. F. (1953), Anhydrite-gypsum equilibrium relations: *Am. Jour. Sci.*, **251**, 884–898.

MAPSTONE, G. E. (1954), The weathering of pyrite: *Chemistry and Industry*, 577–578.

MERWIN, H. E. (1914), The simultaneous crystallization of calcite and certain sulphides of iron, copper and zinc. A crystallographic study: *Am. Jour. Sci.*, 4th ser., **38**, 355–359.

MEUNIER, STANISLAS (1869), Étude minéralogique du fer météorique de Deesa: *Cosmos*, **5**, 581.

MICHEL, ANDRE (1937), Propriétés magnétiques de quelques solutions solides, Chapter III. Le sulfuré ferreux et ses solutions solides: *Annales de Chimie*, 11th ser., **8**, 379–416.

——— (1955), Étude de la réaction de l'hydrogène sulfuré sur les oxydes de fer, pt. I, Étude de la réaction de fixation et du produit de réaction: *Soc. Chimique de France, Bull.*, fasc. **10**, 1187–1188.

——— AND MRS. CHOAIN (1956), Étude de la rèaction de l'hydrogène sulfuré sur les oxydes de fer, pt. III. Réactivite des oxydes de fer anhydres et hydratés. Le phénomène de revivification: *Soc. Chimique de France, Bull.*, fasc. **3**, 453–455.

MILLER, J. P. (1952), A portion of the system calcium carbonate-carbon dioxide-water with geological implications: *Am. Jour. Sci.*, **250**, 161–203.

MILNER, H. B. (1929), Sedimentary petrography, 2d ed., 225, Thomas Murby and Co., London.

——— (1940), Sedimentary petrography, 3d ed., 528, Thomas Murby and Co., London.

OKAZAKI, ATSUSHI AND HIRAKAWA, KINSHIRO (1955). The *x*-ray study of $FeSe_x$, II: *Busseiron Kenkyu* No. **90**, 59–60.

OFTEDAHL, CHR. (1955), On the sulphides of the alum shale in Oslo: *Norsk Geol. Tidsskrift*, **35**, 117–120.

PEHRMANN, GUNNAR (1954), Über den Magnetismus einiger Magnetkiese: *Acta Acad. Aboeniss, Math. et Phys.*, **19**, 3–8.

RICHTER, D. H. AND INGERSON, EARL (1954), Some considerations regarding liquid inclusions as geologic thermometers: *Econ. Geol.*, **49**, 786–789.

RODGERS, JOHN (1940), Distinction between calcite and dolomite on polished surfaces: *Am. Jour. Sci.*, **238**, 788–798.

ROSENTHAL, GERNOT (1956), Versuche zur Darstellung von Markasit, Pyrit, und Magnetkies aus wässrigen Lösungen bei Zimmertemperatur: *Heidelberger Beitr. z. Mineralogie u. Petrographie*, **5**, 146–164.

RUBEY, W. W. (1930), Lithologic studies of fine-grained Upper Cretaceous sedimentary rocks of the Black Hills regions: *U. S. Geol. Survey Prof. Paper* **165-A**, 6–7.

SIDOT, TH. (1868), Sur la préparation des sulfures de fer et de manganèse: *Acad. Sci. Paris Comptes Rendus*, **66,** 1257–1258.

SKINNER, B. J. (1953), Some considerations regarding liquid inclusions as geologic thermometers: *Econ. Geol.*, **48,** 541–550.

SMITH, F. G. (1953), Historical development of inclusion thermometry, Univ. of Toronto Press, Toronto.

SMYTH, C. H., JR. (1911), A new locality of pyrrhotite crystals and their pseudomorphs: *Am. Jour. Sci.*, 4th ser., **32,** 156–160.

SORBY, H. C. (1858), On the microscopical structure of crystals, indicating the origin of minerals and rocks: *Geol. Soc. London Quart. Jour.*, **14,** 453–500.

STANTON, R. L. (1955), The occurrence and paragenesis of pyrrhotite and chalcopyrite in sediments near Rockley, New South Wales: *Royal Soc. New South Wales Jour. and Proc.*, **89,** 73–77.

STELZNER, A. W. (1896), Beiträge zur Enstehung der Freiberger Bleierz und der erzgebirgischen Zinnerz-Gänge: *Zeits. prakt. Geol.*, **4,** 400.

STEVENS, R. E. (1933), The alteration of pyrite to pyrrhotite by alkali sulphide solutions: *Econ. Geol.*, **28,** 1–19.

STROMEYER, FRIEDRICH (1814), Analyse zweier Magnetkiese, und Untersuchungen über den kunstlichen Magnetkies: *Annalen der Physik*, **48,** 183–192.

TAMAYO, ELEONORA (1955), Sur la présence de pyrrhotite de néoformation dans des argiles sédimentaires de Sicile: *Soc. Géol. France, Bull.*, 6th ser., **5,** 375–379.

WASER, JURG (1951), The Lorentz and polarization correction for the Buerger precession method: *Rev. Sci. Inst.*, **22,** 567–568.

WEIL, RENE (1955), Reproduction expérimentale des sulfides métalliques des sédiments biogènes: *Congrès Soc. Savantes Paris, Comptes Rendu, Sciences*, 80th, (**1955**), 117–125.

Manuscript received Sept. 24, 1956.